Please cite the Published Version

Enhanced reversible redox activity of hemin on cellulose microfiber integrated reduced graphene oxide for H$_2$O$_2$ biosensor applications

Selvakumar Palanisamy[a,b*], Vijayalakshmi Velusamy[a**], Shih-Wen Chen[b], Thomas C.K. Yang[b***], Sridharan Balu,[b] Craig E. Banks[c]

[a]Division of Electrical and Electronic Engineering, School of Engineering, Manchester Metropolitan University, Chester Street, Manchester M1 5GD, United Kingdom

[b]Department of Chemical Engineering, National Taipei University of Technology, No. 1, Section 3, Chung-Hsiao East Road, Taipei City, Taiwan (ROC)

[c]School of Science and the Environment, Manchester Metropolitan University, Chester Street, Manchester M1 5GD, United Kingdom

Corresponding authors

* S. Palanisamy (prmselva@gmail.com)

** V. Velusamy (V.Velusamy@mmu.ac.uk)

*** T.C.K. Yang (ckyang@mail.ntut.edu.tw)

Abstract

In recent years, the carbohydrate polymers incorporated composite materials have shown significant interest in the bioanalytical chemistry due to their enhanced catalytic performances of various enzymes or mimics. This paper reports the fabrication of novel H_2O_2 biosensor using a hemin immobilized reduced graphene oxide-cellulose microfiber composite (hemin/RGO-CMF). The RGO-CMF composite was prepared by the reduction of GO-CMF composite using vitamin C as a reducing agent. Various physio-chemical methods have applied for the characterization of RGO-CMF composite. Cyclic voltammetry results revealed that the hemin/RGO-CMF composite shows a better redox electrochemical behavior than hemin/RGO and hemin/GO-CMF. Under optimized conditions, the hemin/RGO-CMF composite exhibit a linear response to H_2O_2 in the concentration range from 0.06 to 540.6 µM with the lower detection limit of 16 nM. The sensor also can able to detect the H_2O_2 in commercial contact lens solution and milk samples with functional recovery, which authenticates the potential ability in practical sensors.

Keywords: Peroxidase mimic; Hemin; Reduced graphene oxide; Cellulose microfibers; Redox electrochemistry; H_2O_2 biosensor

1. Introduction

Hydrogen peroxide (H_2O_2) is one of the most well-known simplest peroxides and plays an essential role in human metabolism and biological functions (Wang, Zhu, Zhuo, Zhu, Papakonstantinou, & Lubarsky, 2013). As a critical oxidizing substance, H_2O_2 has been widely used for various potential applications such as pulp and paper-bleaching, production of organic compounds, wastewater treatment, and cosmetic applications (Seders, Shea, Lemmon, Maurice, & Talley, 2007; Numata, Funazaki, Ito, Asano, & Yano, 1996). Furthermore, due to its robust oxidizing nature, H_2O_2 has been used as either monopropellant (not mixed with fuel) or bipropellant (mixed with fuel) in a rocket (Chan, Liu, Tseng, & Kuo, 2013.). The high exposure level of H_2O_2 can cause the oxidative stress and severe cell damage and can result into cancer, cardiovascular diseases, and neurodegenerative disorders (Alfadda & Sallam, 2012; Kamat & Devasagayam, 2000). Therefore, sensitive and reliable detection of H_2O_2 is drawing much attention in numerous fields. Over the past decades, a wide range of sensitive methods has been used for reliable detection of H_2O_2 such as fluorescence, chemiluminescence, chromatography, spectrophotometry and electrochemical techniques (Feng, Wang, Dang, Xu, Yu, & Zhang, 2017.; Yuan & Shiller, 1999; Almuaibed & Townshend, 1994; Sherino, Mohamad, Nadiah Halim, Suhana & Manan, 2018.). Compared to available traditional chromatographic, spectrophotometric and fluorescence methods, the electrochemical techniques are widely used for the detection of H_2O_2 due to their high sensitivity, portability, and cost-effectiveness (Rismetov, Ivandini, Saepudin, & Einaga, 2014.). Over past few decades, enzymatic and non-enzymatic sensors have been consistently used for accurate detection of H_2O_2 (Chen, Yuan, Chai, & Hu, 2013; Chen, Cai, Ren, Wen, & Zhao, 2012). However, the fabrication of stable H_2O_2 sensors with high selectivity and sensitivity is still challenging for practical applications (Yagati, Lee, Min, & Choi, 2013.). Hence, the fabrication of a highly sensitive, selective and stable sensor for quantification of H_2O_2 is of great interest for practical applications.

Immense attention has been paid to study of direct electron transfer of heme proteins, or artificial heme enzyme mimics owing to its close structural and biological activity against the small molecules

including H_2O_2 (Hu, 2001; Chattopadhyay & Mazumdar, 2001). Furthermore, heme proteins such as hemoglobin, horseradish peroxidase, and cytochrome c based sensors have shown greater interest for the applications in pharmaceutical, chemical, and food industries (Warshel, Sharma, Kato, Xiang, Liu, & Olsson, 2006; Wilson & Hu, 2000). However, these heme biosensors suffer many disadvantages which may limit their practical applications including cost-ineffectiveness, difficulty in purification, less availability and environmental stability (Dong, Luo, & Liu, 2012.). Henceforth, the fabrication of reliable and stable sensors with improved catalytic activity based on synthetic enzymes and inorganic nanomaterials have become a particular interest. For instance, metal and metal alloy nanoparticles, metal oxides/hydroxides, porphyrins and carbon analogous (C60, graphene, and carbon nanotubes) and their composites (Chen, Yuan, Chai, & Hu, 2013; Chen, Cai, Ren, Wen, & Zhao, 2012) have used as an alternative electro-catalyst to enzyme-based sensors for detection of H_2O_2. Among different carbon nanoforms, graphene or reduced form of graphene oxide (RGO) is 2D superlative carbon material, has gained considerable attention in physical science and engineering fields since its discovery in 2004 (Novoselov et al., 2004.; Lee, Wei, Kysar, & Hone, 2008). Also, RGO has used as a promising material for electrocatalytic applications due to its extraordinary and unique physio-chemical properties (Brownson & Banks, 2010). On the other hand, hemin is an iron protoporphyrin and is the main active center of heme redox proteins such as myoglobin, peroxidase enzymes, cytochromes, and hemoglobin (Guo, Deng, Li, Guo, Wang, & Dong, 2011). In addition, hemin has a peroxidase-like activity with large extinction coefficient in the visible-light region, and has been widely used for a selective detection of small molecules such as peroxynitrite (Peteu, Peiris, Gebremichael, & Bayachou, 2010), H_2O_2 (Huang, Hao, Lei, Wu, & Xia, 2014), O_2 (Liang, Song, & Liao, 2011) and NO (Santos et al., 2013). Compared to traditional peroxidase enzyme catalysts, hemin has many advantages in electroanalysis such as less cost-effective, environmentally stable at higher temperatures, does not affected by pH and toxic chemicals (Santos, Rodrigues, Laranjinha, & Barbosa, 2013). Till date, hemin has been successfully immobilized on different micro and nanomaterials through non-covalent or covalent functionalization including functionalized carbon nanotubes, graphene, and

RGO composites (Guo, Li, & Dong, 2011; Chen, Zhao, Bai, & Shi, 2011; Clausen, Duarte, Sartori, Pereira, & Tarley, 2014; Lei, Wu, Huang, Hao, Zhang, & Xia, 2014; Gu, Kong, Chen, Fan, Fang, & Wang, 2016). However, the direct adsorption of hemin on cellulose carbohydrate polymers supported graphene and RGO composites still limited and rarely reported. Our recent studies revealed that cellulose microfibers (CMF) combined graphene composites can improve the direct electrochemistry of iron (hemoglobin) and copper (laccase) redox center containing enzymes due to the high porosity and excellent biocompatibility of CMF (Velusamy et al., 2017; Palanisamy et al., 2017).

In recent years, RGO based cellulose composites have been prepared by various methods including thermal and chemical reduction methods (Nandgaonkar et al., 2014; Luong et al., 2011). However, in the present work, we have synthesized RGO-CMF composite by an environmentally friendly method, where vitamin C used as a reducing agent. Vitamin C is a well-known natural anti-oxidant, and widely used as a reducing agent for the large-scale production of RGO (literature (**Xu, Shi, Ji, Shi, Zhou, Cui, 2015; De Silva, Huang, Joshi, Yoshimura, 2017; Ferna´ndez-Merino et al., 2010; Kanishka, Silva, Huang, Yoshimura, 2018**). Hence, vitamin C assisted synthesis of RGO-CMF composite has many advantageous over previously reported chemically and hydrothermally prepared RGO/cellulosic composites. For instance, the reported synthesis method is highly scalable and environmentally friendly with cost-effectiveness than previously reported RGO/cellulosic composites. Also, the synthesized RGO-CMF composite has high biocompatibility and excellent stability than the reported RGO/cellulosic composites. Despite its unique advantages, the RGO-CMF composite could be used as an ideal electrode material for immbolization of redox active proteins and enzymes. The hemin was used as a model redox active molecule to study the direct electron transfer properties and electrocatalysis of immobilized hemin on RGO-CMF composite. The intrinsic and superior film-forming nature of CMF combined RGO could provide enhanced direct electron transfer and electrocatalysis of immobilized hemin than pristine RGO.

In the present work, we report a novel H_2O_2 sensor based on hemin immobilized RGO-CMF composite (hemin/RGO-CMF) modified electrode. A simple and environmentally friendly method was used for the synthesis of RGO-CMF composite for the first time, wherein vitamin C was used as a reducing agent of GO-CMF composite. The electrochemical redox behavior of hemin has studied on hemin/RGO-CMF composite, hemin/RGO and hemin/GO-CMF composite modified electrodes and discussed. The heterogeneous electron transfer rate constant and surface coverage of the hemin/RGO-CMF composite was calculated and discussed in detail. The advanced sensor showed excellent electro-reduction ability towards H_2O_2 at lower overpotential (-0.2 V). The sensor is highly selective and showed superior analytical performances towards H_2O_2 than previously reported hemin/RGO based sensors.

2. Experimental

2.1. Materials

Hemin (Ferriprotoporphyrin IX chloride from Porcine, 97 wt%) and graphite powder were purchased from Sigma-Aldrich. Cellulose medium microfibers were obtained from Sigma-Aldrich. H_2O_2 (30%) was received from the Wako pure chemical Industries. Dopamine hydrochloride was obtained from O-Smart Company, Taiwan and used as received. All other chemicals including ascorbic acid, uric acid, glucose were purchased from Sigma-Aldrich and used without any additional purifications. 0.1 M phosphate buffer pH 7 was used as a supporting electrolyte and was prepared using 0.1 M Na_2PO_4 and 0.1 M NaH_2PO_4 with ultrapure (resistivity >18.2 MΩ·cm at 25 °C) doubly distilled (DD) water. The pH was adjusted to the desired pH using either diluted H_2SO_4 or NaOH. The ultrapure DD water was used for the preparation of all stock solutions. Commercial contact lens solution (3% H_2O_2) and milk samples were purchased from the supermarket in Taipei, Taiwan. All other chemicals and reagents used in this study is of analytical grade and used without any purification or modification. All the experiments were conducted at room temperature (25 ± 2 °C) unless otherwise stated.

2.2. Characterizations, electrochemical methods, and electrode setup

The surface morphological characterizations of the materials were analyzed using Hitachi S-

4300SE/N High-Resolution Schottky Analytical VP scanning electron microscope. The formation of the GO-CMF and RGO-CMF composites was confirmed using a Fourier transform infrared (FTIR) spectroscopy and was done by JASCO FTIR-6600 spectrometer. Dong Woo 500i Raman spectrometer was used to acquire the Raman spectra of the as-prepared materials. Cyclic voltammetry (CV) and amperometry measurements were carried out using a CHI 1205B electrochemical workstation (CH Instruments). A standard three-electrode setup was used for electrochemical studies, where hemin/ RGO-CMF composites modified glassy carbon electrode (GCE) with a geometrical surface area of 0.079 cm^2 was used as a working electrode, and Saturated Ag|AgCl and Pt wire were used as a reference and counter electrodes, respectively. A rotating disc electrode (RDE) with an apparent surface area same as GCE was used for amperometric measurements. The electrochemically active surface area of the RGO-CMF composites modified electrode was 0.12 cm^2 and was calculated from the CV response of standard ferricyanide system using Randles–Sevcik equation, as reported early (Palanisamy, Wang, Chen, Thirumalraj, & Lou, 2016).

2.3. Synthesis of RGO-CMF composites and immobilization of hemin

The graphite oxide was synthesized using the well-known Hummers method (Hummers & Offeman, 1958). To prepare RGO-CMF composite, first, the graphite oxide powder (0.5 mg mL^{-1}) was added into the CMF solution (5 mg mL^{-1}). The resulting mixture was bath sonicated (25 min) until the apparent suspension of GO-CMF composite obtained. Then, 5 mg of vitamin C (ascorbic acid) was added into the GO-CMF composite suspension and bath stirred in 60ºC until the mixture turns to black color. The resulting RGO-CMF composites composite was centrifuged (g = 1409) and re-dispersed in water for further use. For comparison, the RGO was prepared using the same method mentioned above without CMF. The as-synthesized RGO was re-dispersed in dimethylformamide for new use.
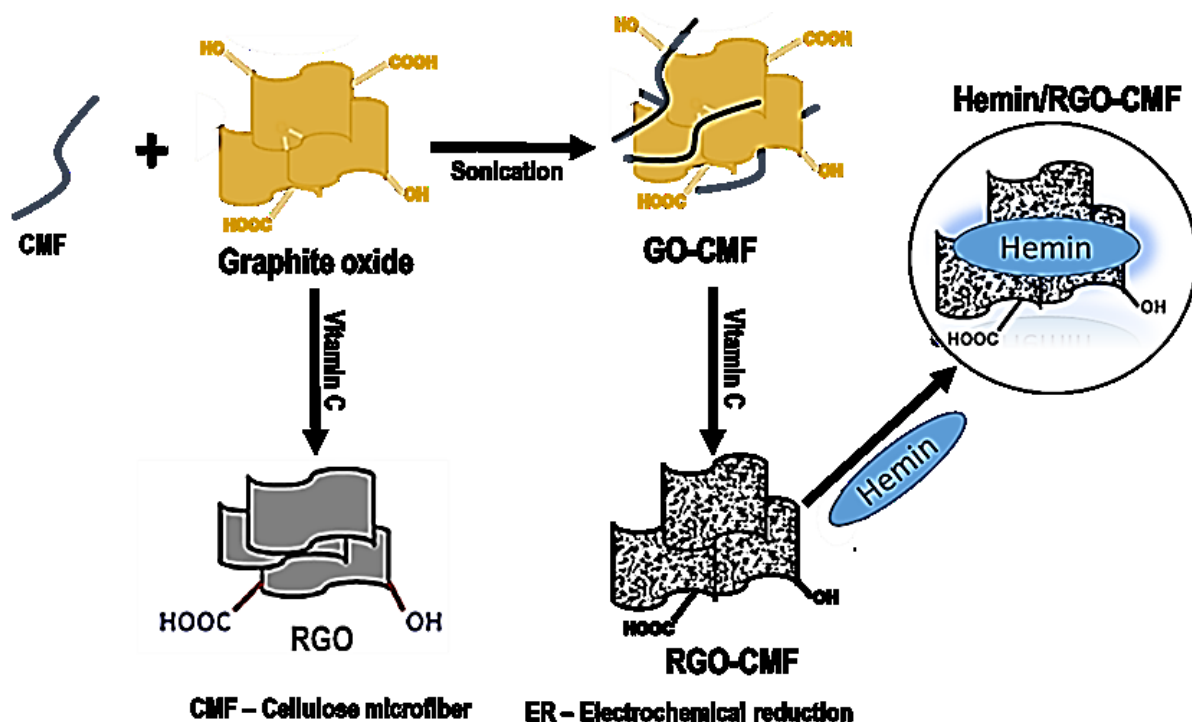
Scheme 1 Schematic representation of the synthesis of GO-CMF composite and fabrication of hemin/RGO-CMF composite sensor.

Before the electrode modification, the glassy carbon electrode was polished with 0.5 µm alumina powder and sonicated in ethanol/water mixture, then dried in an air oven. About 8 µL of as-prepared RGO-CMF composites composite dispersion was dropped on pre-cleaned GCE and air dried. Then, the optimum amount of 8 µL of hemin solution (2 mg mL^{-1}) was drop coated on the RGO-CMF composites modified electrode and allowed to try in an air oven. The fabricated hemin/ RGO-CMF composites modified electrode were used for the further electrochemical studies. The hemin solution (2 mg mL^{-1}) was prepared using 10% liquid ammonia. The hemin, RGO, and hemin/GO-CMF modified electrodes were made by drop coating optimum amount (8 µL) of hemin on bare, RGO and GO-CMF unmodified GCEs. Schematic representation of the synthesis of GO-CMF composite and immobilization of hemin on RGO-CMF composite is shown in **Scheme 1**. The electrochemical measurements were performed in N$_2$ saturated pH 7 unless otherwise stated. The fabricated electrodes were stored in a dry condition when not in use.

3. Results and discussion

3.1. Characterizations of as-prepared materials

The FTIR is a sensitive and most preferred technique that has been widely used for identification of the compounds present in the composite. Furthermore, it has also been widely used to study the interaction of molecules in the composite. **Fig. 1A** displays the typical FTIR spectra of GO, GO-CMF, RGO and RGO-CMF composite. The FTIR spectra of GO (black profile) shows five distinct vibrational bands, namely O–H stretching (3540 cm^{-1}), asymmetric and symmetric CH_2 stretching (2951 cm^{-1}), C=O carbonyl stretching (1630 cm^{-1}) and –OH stretching of C–OH (1203 cm^{-1}). On the other hand, GO-CMF composite (green profile) shows the vibration bands at 3510, 2990, 1675 cm^{-1}, are attributed to the presence of O–H stretching vibrations of hydroxyl groups, carboxyl bending and –CH stretching of a −CH_2 group of cellulose (Velusamy et al., 2017; Kafy, Akther, Zhai, Kim, & Kim, 2017.). The above results confirmed the formation of GO-CMF composite. Nevertheless, the vibration bands for O–H stretching (3540 cm^{-1}) and –OH stretching (1203 cm^{-1}) were decreased in the FTIR spectrum of RGO-CMF composite (red profile) and RGO (blue profile), which indicates the efficient reduction of hydroxyl groups by vitamin C (Unnikrishnan, Palanisamy, & Chen, 2013). The mechanism of GO reduction by vitamin C is already well-known, and been widely discussed in the literature (**Xu, Shi, Ji, Shi, Zhou, Cui, 2015**). According to previous literature and FTIR analysis, the hydroxyl and epoxide groups on the basal planes of the GO sheets were removed by the reaction with hydrogen atoms of vitamin C (SN2 nucleophilic attack). The presence of CMF will prevent the π-π stacking of RGO sheets. However, the RGO-CMF composite shows more intense peaks for O–H than RGO and is due to the presence of CMF in the composite. The results further confirmed the formation of RGO-CMF composite.
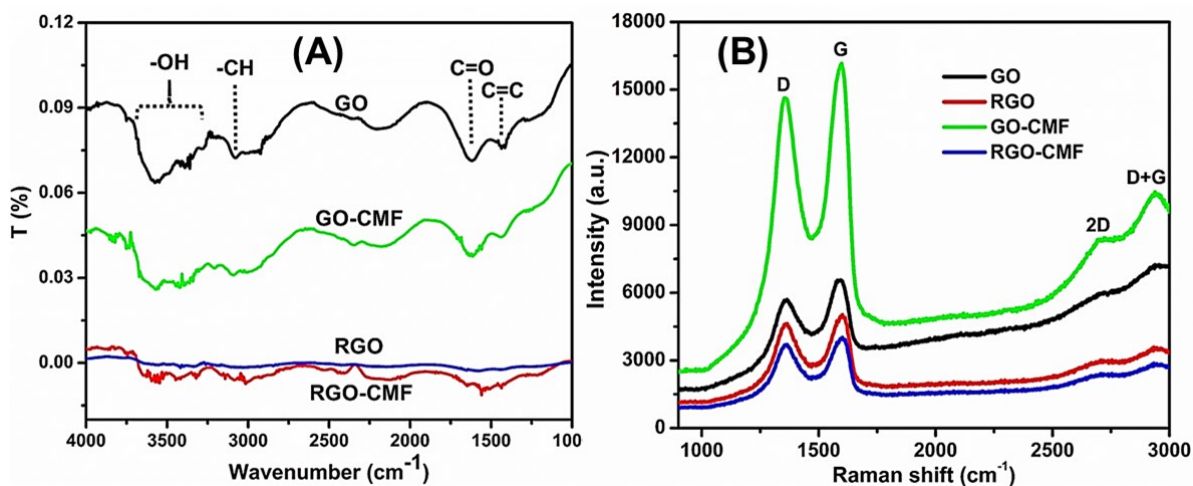
Figure 1 A) FTIR spectra of GO, GO-CMF, RGO and RGO-CMF composite. B) Raman spectra of GO, GO-CMF, RGO, and RGO-CMF.

To further confirm the formation of RGO-CMF composite, Raman spectroscopy is used to characterize the GO, GO-CMF, and RGO-CMF composites and corresponding Raman spectra are shown in **Fig. 1B**, The GO (green profile) and GO-CMF composite (black pattern) show a typical G band at 1598 and 1596 cm^{-1}, is due to the E_{2g} phonon of the sp^2 carbon (Johra, Lee, & Jung, 2014). Also, the D band of GO and GO-CMF composite appeared at 1359 and 1355 cm^{-1}, which is corresponding to the breathing mode of k-point phonons of A_{1g} symmetry. While, the D and G bands of RGO-CMF composite (red profile) appeared at 1346 and 1589 cm^{-1}, respectively. The D and G bands of RGO-CMF composite are shifted to lower when compared to the position of earlier GO and GO-CMF composite, which indicates the formation of defects and amorphous carbon character of the composite. The intensity ratio of D and G bands (I_D/I_G) of GO, GO-CMF, RGO and RGO-CMF composite is further calculated to confirm the transformation of GO to RGO. The I_D/I_G of GO, GO-CMF, RGO and RGO-CMF composite was 0.98, 0.95, 0.91 and 0.92, respectively. The smaller I_D/I_G of RGO-CMF composite indicates that the presence of some edge plane defects with the disorder of aromatic domains (Johra, Lee, & Jung, 2014). The I_D/I_G of RGO-CMF composite was found similar to RGO, which further shows the transformation of GO to RGO. Furthermore, the RGO-CMF composite shows a clear 2D and S3 (D+G) bands at 2699 and 2933 cm^{-1}. The result further confirms that the as-prepared composite has better graphitization and contains few
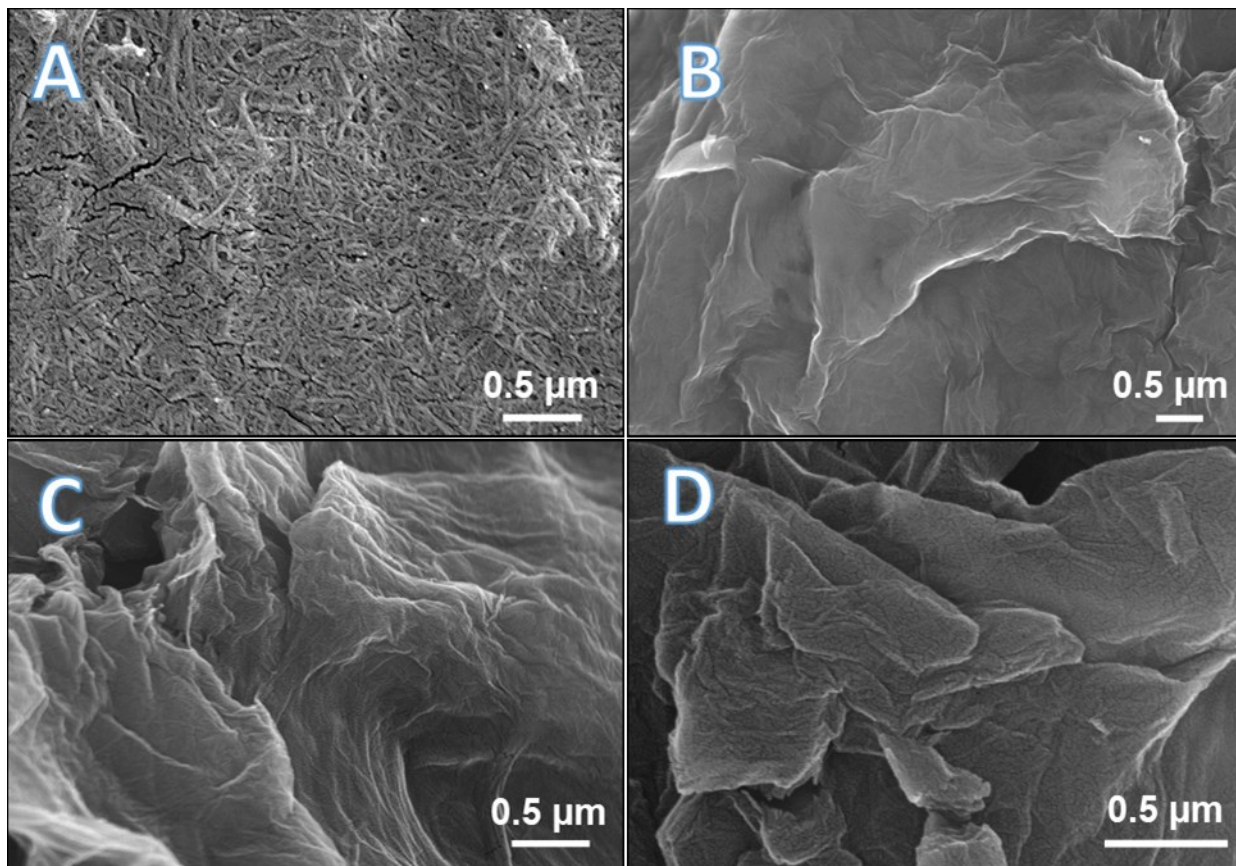
graphene layers with some defects.

Figure 2 High-resolution SEM images of CMF (A), GO (B), RGO (C) and RGO-CMF (D).

The high-resolution scanning electron microscope (SEM) was used to analyze the surface morphology of CMF, GO, GO-CMF and RGO-CMF composite and corresponding SEM images are shown in **Fig. 2**. The surface of CMF (A) reveals the typical dense fiber morphology (**Fig. 2A**), and the GO shows the smooth surface wrinkled morphology (**Fig. 2B**). On the other hand, the RGO (**Fig. 2C**) shows a typical wrinkled morphology and is resulting from the removal of hydroxyl and epoxy groups in the basal planes of GO and restoration the C = C bond. The SEM image of RGO-CMF composite shows crumbled 3D architecture morphology where the dense CMF were absorbed on RGO sheets (**Fig. 2D**). The crumbled 3D architecture morphology of RGO-CMF composite is resulting from the high miscible quality of CMF with RGO, and the strong interaction of CMF with GO during the reduction process. The crumbled 3D architecture morphology of RGO-CMF composite will be more beneficial for the immobilization of hemin on the surface of the composite.

3.2. Redox electrochemistry of hemin at different modified electrodes

The direct electrochemistry of hemin immobilized different modified electrodes were studied using CV. **Fig. 3A** illustrates the CV response of hemin immobilized bare GCE (a), GO-CMF/GCE (b), RGO/GCE (c) and RGO-CMF composite/GCE (e) in N_2 saturated pH 7.0. The CV response of different modified electrodes was investigated in the potential scanning from 0.3 to -0.8 V at a scan rate of 100 mV/s. The hemin immobilized bare (curve a) and GO-CMF composite (curve b) GCEs show an irreversible redox peak (reduction of hemin-Fe) at -0.408 and 0.384 V, which indicates weak adsorption and diminished redox electrochemical behavior of hemin on these modified GCEs. Also, the cathodic current response of hemin immobilized bare, and GO-CMF composite GCEs were 2.63 and 4.31 µA. On the other hand, hemin/RGO modified electrode shows a weak redox couple with a formal potential ($E^{0'}$) of -0.355 V, which ascribed to the redox electrochemical behavior of Fe^{II}/Fe^{III} in immobilized hemin. In addition, the anodic (E_{pa}) and cathodic (E_{pc}) peaks were appeared at – 0.299 and -0.41 V, respectively. The peak-to-peak separation (ΔE_p) of the hemin redox couple was 111 mV. It should be noted that a higher background current of RGO is suggesting the efficient reduction of GO with the high surface area. The RGO-CMF modified electrode did not show any apparent peak in the potential scanning from -0.8 to 0.3 V, while a pair of stable and well-defined redox peaks were observed at hemin immobilized RGO-CMF composite modified electrode. The enhanced redox peaks of hemin were observed at RGO-CMF composite modified electrode than that of hemin/RGO modified electrode. The result implies that the direct electrochemistry of hemin is more favorable on RGO-CMF composite than RGO and other modified electrodes. The E_{pa} and E_{pc} of hemin were observed at -0.278 and -0.383 V, respectively. The ΔE_p of hemin redox couple was 105 V, which is smaller than hemin/RGO modified electrode. The result confirms the fast direct electron transfer of hemin redox-active site and the composite modified electrode. The combined synergy effects of graphene and CMF result in the enhanced direct electron transfer of hemin. The impact of drop coating amount of hemin on RGO-CMF composite was investigated using CV. **Fig. 3A inset** shows the effect of hemin loading on the composite vs. I_{pc} of hemin from the CV response. It can

be seen that 8 μL drop coated hemin modified composite sensor showed an entire current response than others, hence 8 μL hemin drop coated sensor is used as an optimum for further studies.
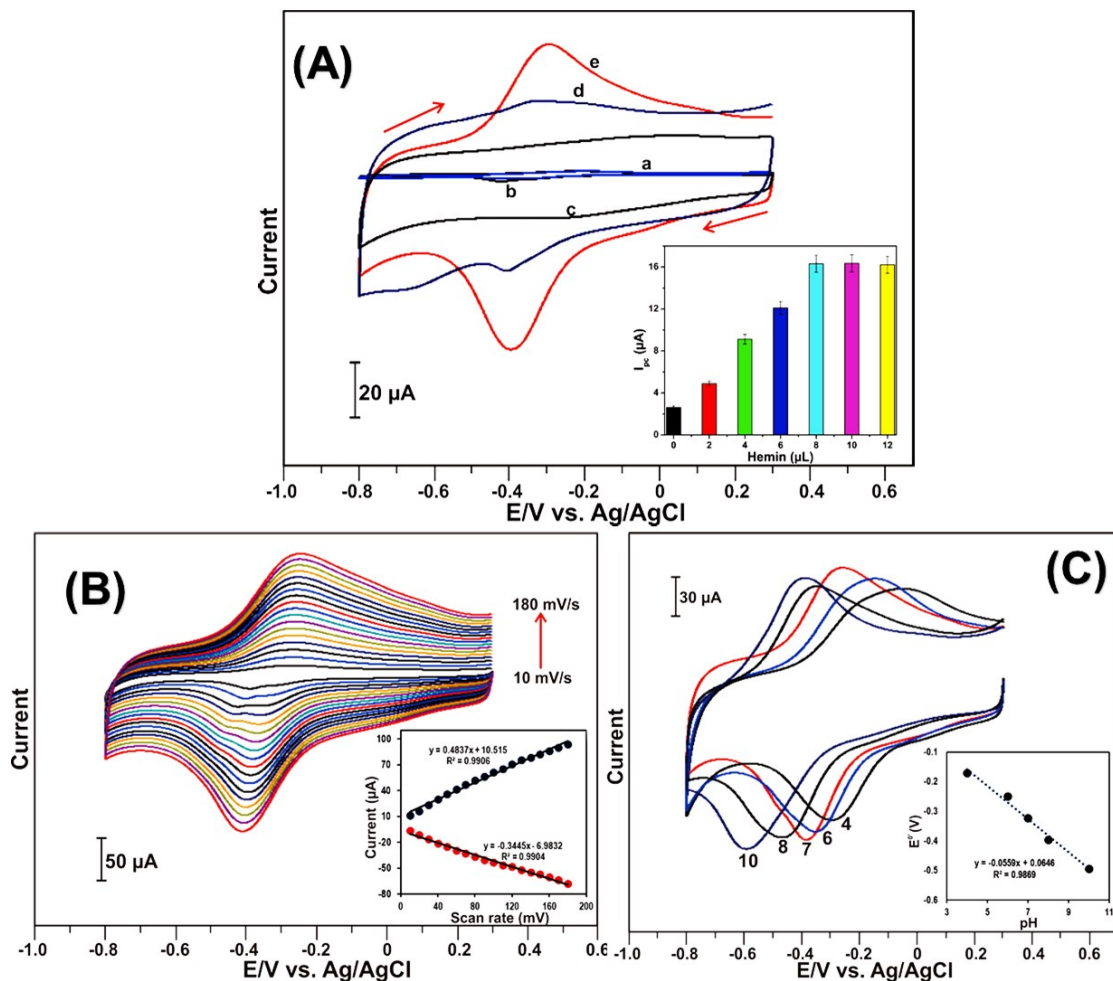

Figure 3 A) CV response of hemin immobilized bare GCE (a), GO-CMF/GCE (b), RGO/GCE (c) and RGO-CMF composite/GCE (e) in the electrochemical cell (pH 7.0) at a scan rate of 100 mV/s. At similar conditions, CV response of RGO-CMF composite modified electrode without hemin. Inset is the effect of loading of hemin on the RGO-CMF composite vs. cathodic peak current (I_{pc}) response of the hemin redox. B) The effect of scan rate on the CV response of hemin immobilized RGO-CMF composite modified GCE in pH 7.0; the scan rate tested from 10 to 180 mV/s (inner to outer). The inset shows the linear dependence of the scan rate vs. anodic (I_{pa}) and cathodic (I_{pc}) current response. C) CVs of hemin immobilized RGO-CMF composite modified GCE in the electrochemical cell containing different pH (pH 3 to 11) at a scan rate of 100 mV/s. The inset shows the linear plot for the formal potential ($E^{0'}$) vs. pH.

We investigated the effect of scan rates on the redox electrochemical behavior of hemin/RGO-CMF composite by CV. **Fig. 3B** shows the CVs of the hemin/RGO-CMF composite at various scan rate (10 to 180 mV/s in N_2 saturated pH 7.0. The CVs shows that the redox peak currents increased upon increasing the scan rates from 10 to 180 mV/s. The redox peak currents of hemin had a linear dependence with the function of scan rates as shown in **Fig.3B inset**. The result indicates that the electrochemical redox behavior of hemin at RGO-CMF composite is a surface-controlled process. In such a surface controlled process, the surface concentration (Γ^*) of the composite can be easily calculated using the Laviron equation (Laviron, 1979a), as shown below.

$$I_p = \frac{n^2 F^2 \nu \Gamma^* A}{4RT}$$

Where n is the number of electrons transferred (n=1) in the hemin redox reaction, F is the Faraday constant (96 485.332 89 C mol^{-1}), n is the scan rate, A is the active surface area (0.12 cm^2), R is the gas constant, and T is the temperature (298.15 K). Thus, Γ^* of the hemin/RGO-CMF composite modified electrode is calculated as 4.26 × 10^{-9} mol cm^{-2} from the slope of I_p vs. scan rate (n). The obtained Γ^* value of the hemin/RGO-CMF composite modified electrode is larger than the reported theoretical value (Sagara, Takagi, & Niki, 1993.) of monolayer coverage of hemin (6.89 × 10^{-11} mol cm^{-2}). The result confirms the effective immobilization of hemin on RGO-CMF composite.

The electron transfer rate constant (*Ks*) of immobilized hemin on RGO-CMF composite electrode could be readily determined using Laviron theory for the surface controlled electrochemical redox system. The *Ks* of the hemin/ RGO-CMF composite electrode was estimated to be 6.87 s^{-1} (n=10) using the following Laviron Eqn (Laviron, 1979b).

$$log\ Ks = \alpha \log (1 - \alpha) + (1 - \alpha) \log \alpha - \log\left(\frac{RT}{nF\nu}\right) - \alpha \frac{(1 - \alpha)nF\Delta E_p}{2.3\ RT}$$

Where α is electron-transfer coefficient (0.5), ΔEp is the peak-to-peak separation of the hemin redox couple (ΔE$_p$ is equal or more than 200 mV since hemin redox is a single electron and proton transfer reaction), n is number of electrons transferred in the hemin redox reaction (n=1), and all other symbols are usual meanings. The calculated Ks value of hemin/RGO-CMF composite electrode is much higher

than the previously reported hemin-graphene, and carbon nanotube composites modified electrodes, as discussed in earlier work (Santos, Rodrigues, Laranjinha, & Barbosa, 2013). The result further indicates that the enhanced direct electron transfers of immobilized hemin on RGO-CMF composite electrode surface.

To better understanding, the redox chemistry of immobilized hemin, the effect of pH on the redox electrochemical behavior of hemin/RGO-CMF composite was studied by CV. **Fig. 3C** shows the typical CV responses obtained for hemin/RGO-CMF composite modified electrode in different pH (pH 4.0, 6.0, 7.0, 8.0, 10.0) at a scan rate of 100 mV/s. A well-defined redox couple with an identical current intensity of hemin is observed in pH 4.0, 6.0, 7.0 and 8.0, which indicates the better pH tolerance. Also, the redox peak potential of hemin shifted towards the negative and positive side upon increasing and decreasing the pH, which shows the effective involvement of protons (H^+) in the redox reaction of hemin. **Fig. 3C inset** shows that the $E^{0'}$ of the immobilized hemin had a linear dependence on the pH, and the slope and correlation coefficient (R^2) values were −55.9 mV/pH and 0.9869, respectively. The obtained slope value of the immobilized hemin is close relationship to the reported theoretical value (−58.6 mV/pH) for an equal number of protons (H^+) and electrons (e^-) involving redox process (Laviron, 1979b). Hence, the redox electrochemical reaction of hemin on RGO-CMF composite modified electrode is involving an equal number of protons and electrons (**Fig. 4B**).

3.3. Electro-catalysis of immobilized hemin and amperometric determination of H_2O_2

We studied the electro-catalysis and electro-reduction ability of hemin/RGO-CMF composite modified electrode towards H_2O_2. **Fig. 4A** shows the typical CV response of hemin/RGO-CMF composite modified electrode in the absence (a) and presence of 1 mM H_2O_2 (b) in N_2 saturated pH 7.0 at a scan rate of 100 mV/s. A well-defined redox peak was observed for the hemin/RGO-CMF composite in the absence of H_2O_2. While, the cathodic peak of the hemin redox couple dramatically increased in the presence of H_2O_2, which is resulting from the reduction of H_2O_2 by immobilized hemin on the composite modified electrode. Also, the reduction peak of H_2O_2 occurred at more positive potential (-0.17 V) than

the original cathodic peak (-0.38 V) of hemin redox couple, which further shows the excellent electro-catalysis of immobilized hemin. The excellent electro-reduction ability of H_2O_2 is due to the excellent catalytic activity of immobilized hemin on RGO-CMF composite. The combined unique properties (high conductivity, large porous nature, and high surface area) and synergy effect of RGO-CMF was also a core reason for the firm attachment of more hemin molecules and the lower-reduction potential ability of H_2O_2. The possible mechanism of electro-reduction of H_2O_2 by the hemin/RGO-CMF composite has shown in **Fig. 4B**. The electro-reduction mechanism of H_2O_2 by hemin on different modifiers have already been discussed widely, henceforth a simplified mechanism of H_2O_2 reduction by hemin/RGO-CMF composite modified electrode can be written as follow
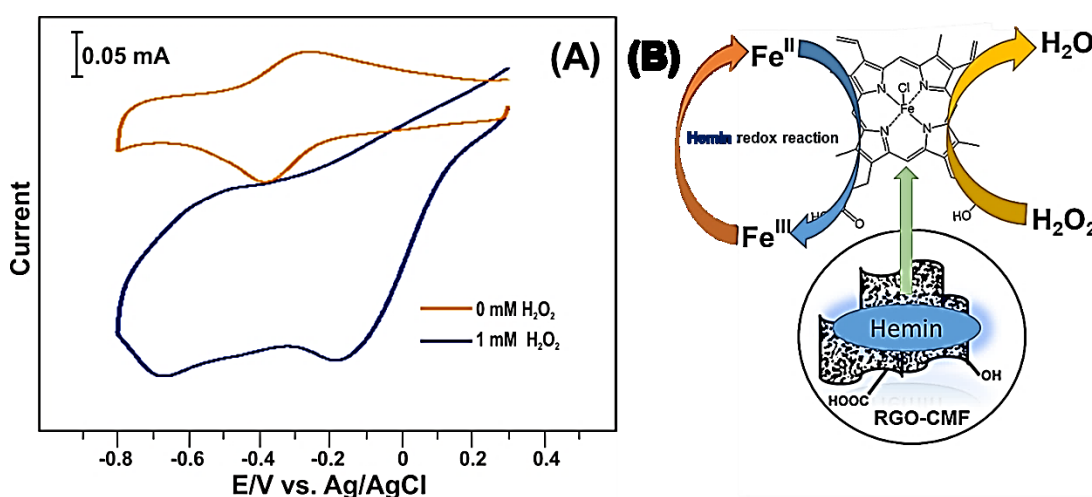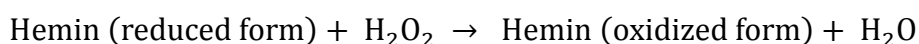
$$\text{Hemin (reduced form)} + H_2O_2 \rightarrow \text{Hemin (oxidized form)} + H_2O$$

Figure 4 A) CV response of the hemin/RGO-CMF sensor in the absence (a) and presence of 1 mM H_2O_2 into the N_2 saturated pH 7.0 at a scan rate of 100 mV/s. B) The electro-reduction mechanism of H_2O_2 on the hemin/RGO-CMF sensor surface.

The amperometric *i-t* method is used for the accurate and fast detection of H_2O_2 since it is an ideal method for the determination of H_2O_2 using redox active enzyme/mimics modified sensors. Also, this method offers more sensitivity and lower background current than available other voltammetric methods. **Fig. 5** displays a typical real-time amperometric response of hemin/RGO-CMF composite modified RDE for the different concentration additions of H_2O_2 (from 0.06 to 685.1 µM) into the constantly stirred pH 7.0

at different intervals. The amperometric measurements were carried out with an optimum applied potential (E_{app}) of -0.2 V. As shown in **Fig. S1**, a maximum amperometric current response of 1 µM H_2O_2 was observed for E_{app} = -0.2 V. The sensor showed less sensitivity towards H_2O_2 when the E_{app} was above or below -0.2 V. Hence, E_{app} of -0.2 V is used as an optimum for the sensitive determination of H_2O_2 using the modified sensor.
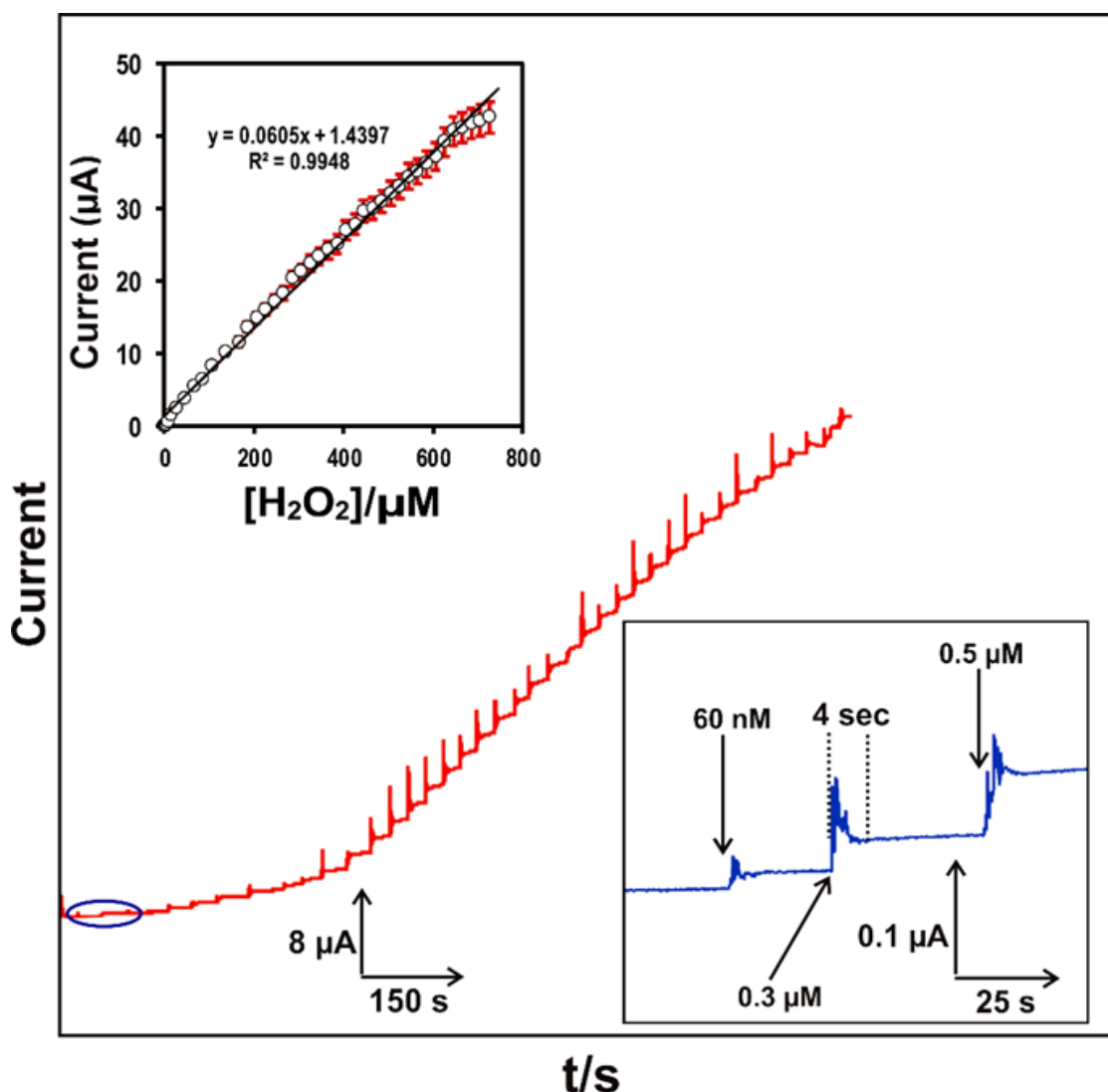

Figure 5 Amperometric real-time current response of hemin immobilized RGO-CMF composite modified RDE for the additions of different concentration of H_2O_2 (0.06 to 865.1 µM) into the pH 7.0 with an applied potential of -0.2 V. The lower inset shows the enlarged version of the amperometric sensor response for the addition of 60 nM, 300 nM, and 500 nM H_2O_2 into the pH 7.0. The linear calibration plot for [H_2O_2] vs. current response (upper inset).

It can be seen that the hemin/RGO-CMF modified electrode shows a stable and well-defined amperometric response for the addition of different concentration of H_2O_2 into the pH 7.0. As shown in **Fig. 5 lower inset**, the hemin/RGO-CMF modified electrode exhibits a clear response to the addition of 60, 300 and 500 nM H_2O_2, which shows its excellent electro-reduction ability of the composite modified electrode towards H_2O_2. Also, the sensor reaches its 95% steady-state current (defined as response time) towards H_2O_2 within 4 s (**Fig. 5 lower inset**), indicating the fast electrocatalytic reduction reaction of the sensor towards H_2O_2. One can see that the amperometric current response increases with increasing the concentration of H_2O_2. The response of the sensor was linear over the concentration of H_2O_2 from 0.06 to 540.6 μM with an R^2 of 0.9904. (**Fig. 5 upper inset**). The linear regression equation of the calibration plot is expressed as follows

$$I\ (\mu A) = 0.0605 + 1.4397\ C\ (\mu M)$$

The limit of the detection (LOD) of the sensor was calculated to be 16 nM based on S/N = 3. The sensitivity of the sensor was calculated to be 0.51 $\mu A \mu A^{-1}\ cm^{-2}$. The LOD, E_{app} and linear response range of the fabricated sensor were compared with previously reported hemin based H_2O_2 sensors. The comparative results are shown in **Table ST1**. The comparison table clearly shows that the hemin/RGO-CMF composite modified electrode has greater analytical performance (including lower LOD, wider linear response range, and lower working potential) towards the determination of H_2O_2 than that of previously reported hemin based sensors, as shown in **Table ST1**. It is also worthy to note that the hemin/RGO-CMF composite modified electrode has more Γ* with high stability (up to 42 days) than previously reported hemin based H_2O_2 sensors including rGO and graphene composites, (**Table ST1**). The enhanced analytical performances and high stability of the sensor are resulting from the high catalytic nature of immobilized hemin and the combined synergetic effects of RGO-CMF composite. Hence, the hemin/RGO-CMF composite sensor can be used as an advanced material for sensitive and low-levels detection of the H_2O_2.

The selectivity of the hemin/RGO-CMF composite sensor towards the detection of H_2O_2 in the presence of potentially interfering compounds was examined by the amperometric i-t method. The interfering species such as ascorbic acid (AA), dopamine (DA), glucose (Glu), uric acid (UA), Cu^{2+}, Ni^{2+}, Cd^{2+}, and Na^+ was chosen for selectivity studies, since these compounds may act on the fabricated electrode surface due to their closer oxidation/reduction potential. **Fig. S2** shows the amperometric response of the hemin/RGO-CMF composite sensor for the addition of 0.5 µM H_2O_2 and 50 µM additions of ascorbic acid (AA), dopamine (DA), glucose (Glu), uric acid (UA), Cu^{2+}, Ni^{2+}, $Cd^{2+,}$ and Na^+) into the N_2 saturated pH 7.0. The working potential held at -0.2 V. The hemin/RGO-CMF composite sensor shows a clear amperometric response for the addition of 0.5 µM H_2O_2, whereas the 50 µM additions of aforementioned interfering species did not show any apparent reaction on the modified electrode. Furthermore, a stable amperometric response for the subsequent additions of 0.5 µM H_2O_2 into the pH 7.0. The result clearly shows the highly selective nature of developed hemin sensor for the detection of H_2O_2 in the presence of 100 fold concentrations of common interfering species. Hence, the hemin/RGO-CMF composite modified electrode can be used as a selective sensor for the detection of H_2O_2.

The storage stability of the hemin/RGO-CMF composite sensor towards detection of H_2O_2 was investigated using amperometry. The storage stability of the sensor was examined from the amperometric response of 0.5 µM H_2O_2 and was repeated periodically up to 42 days. The experimental conditions are similar to of in **Fig. 5**. The hemin/RGO-CMF composite sensor was stored at room temperature (25 ± 2ºC) when not in use. The obtained stability results of the sensor are summarized in **Fig. S3**. The hemin/RGO-CMF composite sensor retains 96.2% of the initial sensitivity to H_2O_2 after 11 days. Also, the sensor only lost 17.1% of the initial response of H_2O_2 after 42 days, revealing the excellent storage stability of the developed sensor. To further check the accuracy and precision of the developed sensor, the repeatability and reproducibility of the sensor were investigated using CV. The experimental conditions are similar to **Fig. 4A**. The relative standard deviation (RSD) of 4.8% was found for a single sensor electrode for the measurement in 8 different samples containing pH 7.0 with 1 mM H_2O_2. The 5

independently prepared sensors showed good reproducibility for detection of 1 mM H_2O_2 with an RSD of 2.8%. The result reveals that the hemin/RGO-CMF composite sensor has excellent repeatability and reproducibility with excellent storage stability, which attributed to the excellent biocompatibility and synergistic effect of the RGO-CMF composite.

The practical ability of hemin/RGO-CMF composite sensor was evaluated in H_2O_2 containing commercially available contact lens cleaning solution and milk samples. Amperometry *i-t* method was used for the detection of H_2O_2, and experimental conditions are the same as in **Fig. 5**. The standard addition method was used to calculate the recovery of H_2O_2 in contact lens cleaning solution and milk samples. Before the experiments, the contact lens cleaning solution was diluted with pH 7.0 to obtain the desired H_2O_2 concentration. The unknown and known concentration of H_2O_2 containing contact lens solution samples were used for real sample analysis. Likewise, the known concentration (5 µM) of H_2O_2 containing milk sample was handled for the actual sample analysis. The obtained recovery of H_2O_2 in contact lens cleaning solution and milk sample is tabulated in **Table ST2**. The hemin/RGO-CMF composite sensor shows a 98.7 and 98.4% recovery of H_2O_2 in contact lens cleaning solution and milk samples, respectively. The result is revealing the excellent practicality of the developed sensor towards the determination of H_2O_2.

4. Conclusions

In conclusion, a novel and the robust H_2O_2 sensor were reported based on the hemin/RGO-CMF composite modified electrode. A facile and environmental friendly Vitamin C assisted method was used for the synthesis of RGO-CMF composite, and different physio-chemical characterizations confirmed the synthesized materials. Compared with hemin/RGO and hemin/GO-CMF modified electrodes, hemin/RGO-CMF composite modified electrode shows an improved redox electrochemical behavior to hemin, thus resulted to the larger surface concentration and fast electron transfer kinetics of hemin. The fabricated sensor showed a broader linear response (0.06–540.6 µM), lower LOD (16 nM) with appropriate sensitivity for the determination of H_2O_2. The analytical performances of the hemin/RGO-

CMF composite modified electrode were better than previously reported hemin combined graphene, RGO and carbon nanotubes composites based H_2O_2 sensors, which revealed the promising nature of the novel H_2O_2 sensor. In addition to analytical performances, the fabricated H_2O_2 sensor showed a fast response time (4 s), excellent selectivity, high stability, excellent practicality along with appropriate reproducibility and repeatability. As a future perspective, the reported RGO-CMF composite may use as a promising electrode material for immobilization of other redox active enzymes and fabrication of biosensors.

5. Conflicts of interest

The author(s) declare that they have no competing interests

References

Alfadda, A. A., & Sallam, R. M. 2012. Reactive oxygen species in health and disease. Journal of biomedicine and biotechnology, 2012, 936486.

Almuaibed, A. M., & Townshend, A. 1994. Flow spectrophotometric method for determination of hydrogen peroxide using a cation exchanger for preconcentration. Analytica Chimica Acta, 295, 159-163.

Brownson, D. A. C., & Banks, C. E. 2010. Graphene electrochemistry: an overview of potential applications. Analyst, 135, 2768-2778.

Cao, H., Sun, X., Zhang, Y., Hu, C., & Jia, N. 2012. Electrochemical sensing based on hemin-ordered mesoporous carbon nanocomposites for hydrogen peroxide. Analytical Methods, 4, 2412–2416.

Cao, Y., Si, W., Hao, Q., Li, Z., Lei, W., Xia, X., et al. 2018. One-pot fabrication of Hemin-NC composite with enhanced electrocatalysis and application to H_2O_2 sensing. Electrochimica Acta, 261, 206–213.

Chan, Y. A., Liu, H. J., Tseng, K. C., & Kuo, T. C. 2013. Preliminary development of a hydrogen peroxide thruster. World Academy of Science, Engineering and Technology, 7(7), 16467.

Chattopadhyay, K., & Mazumdar, S. 2001. Direct electrochemistry of heme proteins: effect of electrode surface modification by neutral surfactants. Bioelectrochemistry, 53, 17-24.

Chen, J., Zhao, L., Bai, H., & Shi, G. 2011. Electrochemical detection of dioxygen and hydrogen peroxide by hemin immobilized on chemically converted graphene. Journal of Electroanalytical Chemistry, 657, 34–38.

Chen, S., Yuan, R., Chai, Y., & Hu, F. 2013. Electrochemical sensing of hydrogen peroxide using metal nanoparticles: A review. Microchimica Acta, 180, 15–32.

Chen, W., Cai, S., Ren, Q. Q., Wen, W., & Zhao, Y.D. 2012. Recent advances in electrochemical sensing for hydrogen peroxide: a review. Analyst, 137, 49–58.

Clausen, D. N., Duarte, E. H., Sartori, E. R., Pereira, A. C., & Tarley, C. R. T. 2014. Evaluation of a multi-walled carbon nanotube hemin composite for the voltammetric determination of hydrogen peroxide in dental products. Analytical Letters, 47, 750–762.

De Silva, K.K.H., Huang, H.-H., Joshi, R.K., Yoshimura, M., 2017. Chemical reduction of graphene oxide using green reductants. Carbon 119, 190¬-199.

Dong, Z. Y., Luo, Q., & Liu, J.Q. 2012. Artificial enzymes based on supramolecular scaffolds. Chemical Society Reviews, 41, 7890–7908.

Feng, C., Wang, F., Dang, Y., Xu, Z., Yu, H., & Zhang, W. 2017. A self-assembled ratiometric polymeric nanoprobe for highly selective fluorescence detection of hydrogen peroxide. Langmuir, 2017, 33 (13), 3287–3295.

Ferna´ndez-Merino, M.J., Guardia, L., Paredes, J. I., Villar-Rodil, S., Solı´s-Ferna´ndez, P., Martı´nez-Alonso, A., et al. 2010. Vitamin C Is an ideal substitute for hydrazine in the reduction of graphene oxide suspensions. Journal of Physical Chemistry C, 114, 6426–6432.

Gu, C., Kong, F., Chen, Z., Fan, D., Fang, H., & Wang, W. 2016. Reduced graphene oxide-Hemin-Au nanohybrids: Facile one-pot synthesis and enhanced electrocatalytic activity towards the reduction of hydrogen peroxide. Biosensors and Bioelectronics, 78, 300–307.

Gu, T. T., Wu, X. M., Dong, Y. M., & Wang, G. L. 2015. Novel photoelectrochemical hydrogen peroxide sensor based on hemin sensitized nanoporous NiO based photocathode. Journal of Electroanalytical Chemistry, 759, 27–31.

Guo, Y., Deng, L., Li, J., Guo, S., Wang, E., & Dong, S. 2011. Hemin−graphene hybrid nanosheets with intrinsic peroxidase-like activity for label-free colorimetric detection of single-nucleotide polymorphism. ACS Nano, 5, 1282–1290.

Guo, Y., Li, J., & Dong, S. 2011. Hemin functionalized graphene nanosheets-based dual biosensor platforms for hydrogen peroxide and glucose. Sensors and Actuators B: Chemical, 160, 295–300.

Hu, N. 2001. Direct electrochemistry of redox proteins or enzymes at various film electrodes and their possible applications in monitoring some pollutants. Pure and Applied Chemistry, 73, 1979–1991.

Huang, W., Hao, Q., Lei, W., Wu, L., & Xia, X. 2014. Polypyrrole-hemin-reduce graphene oxide: rapid synthesis and enhanced electrocatalytic activity towards the reduction of hydrogen peroxide. Materials Research Express, 1, 045601.

Hummers, W. S., & Offeman, R. E. 1958. Preparation of Graphitic Oxide. Journal of the American Chemical Society, 80, 1339–1339.

Johra, F. T., Lee, J. W., & Jung, W. G. 2014. Facile and safe graphene preparation on solution based platform. Journal of Industrial and Engineering Chemistry, 20, 2883–2887.

Kafy, A., Akther, A., Zhai, L., Kim, H. C., & Kim, J. 2017. Porous cellulose/graphene oxide nanocomposite as flexible and renewable electrode material for supercapacitor. Synthetic Metals. 223, 94–100.

Kamat, P. J., & Devasagayam, T. P. A. 2000. Oxidative damage to mitochondria in normal and cancer tissues, and its modulation. Toxicology, 155, 73−82.

Kanishka, K., Silva, H.D., Huang, H.-H., Yoshimura, M. 2018. Progress of reduction of graphene oxide by ascorbic acid. Applied Surface Science, 447, 338–346.

Laviron, E. 1979a. The use of linear potential sweep voltammetry and of A.C. voltammetry for the study of the surface electrochemical reaction of strongly adsorbed systems and of redox modified electrodes. Journal of Electroanalytical Chemistry and Interfacial Electrochemistry, 100, 263–270.

Laviron, E. 1979b. General expression of the linear potential sweep voltammogram in the case of diffusionless electrochemical systems. Journal of Electroanalytical Chemistry and Interfacial Electrochemistry, 101 (1979b), pp. 19-28.

Lee, C., Wei, X., Kysar, J. W., & Hone, J. 2008. Measurement of the elastic properties and intrinsic strength of monolayer graphene. Science, 321, 385–388.

Lei, W., Wu, L., Huang, W., Hao, Q., Zhang, Y., & Xia, X. 2014. Microwave-assisted synthesis of hemin–graphene/poly(3,4-ethylenedioxythiophene) nanocomposite for a biomimetic hydrogen peroxide biosensor. Journal of Materials Chemistry B, 2, 4324–4330.

Liang, Z. X., Song, H. Y., & Liao, S. J. 2011. Hemin: A highly effective electrocatalyst mediating the oxygen reduction reaction. Journal of Physical Chemistry C, 115, 2604–2610.

Luong, N. D., Pahimanolis, N., Hippi, U., Korhonen, J. T., Ruokolainen, J., Johansson, L.-S., et al. 2011. Graphene/cellulose nanocomposite paper with high electrical and mechanical performances. Journal of Materials Chemistry, 21, 13991–13998.

Nandgaonkar, A. G., Wang, Q., Fu, K., Krause, W. K., Wei, Q., Gorga, R., et al. 2014. A one-pot biosynthesis of reduced graphene oxide (RGO)/bacterial cellulose (BC) nanocomposites. Green Chemistry, 16, 3195–3201.

Novoselov, K. S., Geim, A. K., Morozov, S. V., Jiang, D., Zhang, Y., Dubonos, S. V., et al, 2004. Electric field effect in atomically thin carbon films. Science, 306, 666–669.

Numata, M., Funazaki, N., Ito, S., Asano Y., & Yano, Y. 1996. Flow-injection analysis for hypoxanthine in meat with dissolved oxygen detector and enzyme reactor. Talanta, 43, 2053–2059.

Palanisamy, S., Ramaraj, S. K., Chen, S. M., Yang, T. C. K., Fan, P. Y., Chen, T. W., et al. 2017. A novel laccase biosensor based on laccase immobilized graphene-cellulose microfiber composite

modified screen-printed carbon electrode for sensitive determination of catechol. Scientific Reports, 7, 41214.

Palanisamy, S., Wang, Y. T., Chen, S. M., Thirumalraj, B., & Lou, B. S. 2016. Direct electrochemistry of immobilized hemoglobin and sensing of bromate at a glassy carbon electrode modified with graphene and β-cyclodextrin. Microchimica Acta, 183, 1953-1961.

Peteu, S., Peiris, P., Gebremichael, E., & Bayachou, M. 2010. Nanostructured poly(3,4-ethylenedioxythiophene)–metalloporphyrin films: Improved catalytic detection of peroxynitrite. Biosensors and Bioelectronics, 25, 1914–1921.

Rismetov, B., Ivandini, T.A., Saepudin, E., & Einaga, Y. 2014. Electrochemical detection of hydrogen peroxide at platinum-modified diamond electrodes for an application in melamine strip tests. Diamond and Related Materials, 48, 88–95.

Sagara, T., Takagi, S., & Niki, K.1993. Electroreflectance study of hemin adsorbed on a pyrolytic graphite electrode surface and its coadsorption with methylene blue. Journal of Electroanalytical Chemistry, 349, 159–171.

Santos, R. M., Rodrigues, M. S., Laranjinha, J., & Barbosa, R. M. 2013. Biomimetic sensor based on hemin/carbon nanotubes/chitosan modified microelectrode for nitric oxide measurement in the brain. Biosensors and Bioelectronics, 44, 152–159.

Seders, L. A., Shea, C. A., Lemmon, M. D., Maurice, P. A., & Talley, J. W. 2007. LakeNet: An integrated sensor network for environmental sensing in lakes. Environmental Engineering Science, 24, 183.

Sherino, B., Mohamad, S., Nadiah S., Halim, A., Suhana N., & Manan, A. 2018. Electrochemical detection of hydrogen peroxide on a new microporous Ni–metal organic framework material-carbon paste electrode. Sensors and Actuators B: Chemical, 254, 1148–1156.

Unnikrishnan, B., Palanisamy, S., & Chen, S. M. 2013. A simple electrochemical approach to fabricate a glucose biosensor based on graphene–glucose oxidase biocomposite. Biosensors and Bioelectronics, 39, 70-75.

Velusamy, V., Palanisamy, S., Chen, S. M., Chen, T. W., Selvam, S., Ramaraj, S. K., et al. 2017. Graphene dispersed cellulose microfibers composite for efficient immobilization of hemoglobin and selective biosensor for detection of hydrogen peroxide. Sensors and Actuators B: Chemical, 252, 175-182.

Wang, L., Yang, H., He, J., Zhang, Y., Yu, J., & Song, Y. 2016. Cu-hemin metal-organic-frameworks/chitosan-reduced graphene oxide nanocomposites with peroxidase-like bioactivity for electrochemical sensing. Electrochimica Acta, 213, 691–697.

Wang, T. Y., Zhu, H. C., Zhuo, J. Q., Zhu, Z. W., Papakonstantinou, P., Lubarsky, G., et al. 2013. Biosensor based on ultrasmall MoS_2 nanoparticles for electrochemical detection of H_2O_2 released by cells at the nanomolar Level. Anal. Chem. 85, 10289–10295.

Warshel, A., Sharma, P. K., Kato, M., Xiang, Y., Liu, H., & Olsson, M. H. 2006. Electrostatic basis for enzyme catalysis. Chemical Reviews, 106, 3210–3235.

Wilson, G. S., & Hu, Y. B. 2000. Enzyme-based biosensors for in vivo measurements. Chemical Reviews, 100, 2693–2704.

Xu, C., Shi, X., Ji, A., Shi, L., Zhou, C., Cui, Y. 2015. Fabrication and characteristics of reduced graphene oxide produced with different green reductants. PLoS ONE 10(12), e0144842.

Yagati, A. K., Lee, T., Min, J., & Choi, J. W. 2013. An enzymatic biosensor for hydrogen peroxide based on CeO_2 nanostructure electrodeposited on ITO surface. Biosensors and Bioelectronics, 47, 385-390.

Yuan, J., & Shiller, A. M., 1999. Determination of subnanomolar levels of hydrogen peroxide in seawater by reagent-injection chemiluminescence detection. Analytical Chemistry, 71, 1975-1980.

Zhang, M., Huang, Z., Zhou, G., Zhu, L., Feng, Y., Lin, T., et al. 2015. A sensitive hydrogen peroxide sensor based on a three-dimensional N-doped carbon nanotube-hemin modified electrode. Analytical Methods, 7, 8439–8444.